Smart Rock Technology for Real-time Monitoring of Bridge Scour and Riprap Effectiveness – Design Guidelines and Visualization Tools (Progress Report No. 5)

Contract No: OASRTRS-14-H-MST
(Missouri University of Science and Technology)

Reporting Period: October 1 – December 31, 2015

PI: Genda Chen

Program Manager: Mr. Caesar Singh

Submission Date: January 15, 2016

TABLE OF CONTENTS

EXECUTIVE SUMMARY

In the fifth quarter of this project, field demonstration tests were carried out at the I-44W Roubidoux Creek Bridge (No. L0093), Missouri. The accuracy of the smart rock localization algorithm was validated through field test data.

I - TECHNICAL STATUS

I.1 ACCOMPLISHMENTS BY MILESTONE

In this quarter, field demonstration tests were conducted at the I-44W Roubidoux Creek Bridge (No. L0039), MO. One smart rock with two stacked magnets in automatically pointing to upward system (APUS) was deployed around the downstream side of Bent 7. The test 'crane' was used to facilitate the three-dimensional movement of a 3-axis magnetometer around the deployed smart rock. The 3-axis flux magnetometer sensor head mounted on the test crane was used to measure the magnetic field around the smart rock. To determine the location of each measurement point by means of a total station (survey equipment), a prism was mounted on the crane in proximity to the magnetometer sensor. In addition, a sonar instrument installed on the side of a small boat was employed to map the river bed profile around Bent 7. Finally, the localization of smart rock was performed from the collected magnetic field data and measurement point coordinates.

Task 3.1 Time- and Event-based Field Measurements

In this task, field demonstration tests were carried out on the deck of I-44W Roubidoux Creek Bridge as shown in Figure 1. The river bed profile was mapped by a sonar system. One smart rock was deployed around the downstream side of Bent 7 for bridge scour monitoring. The test crane with a mounted magnetometer sensor was employed to facilitate measurements of the intensity and direction of the magnetic ambient field and the total field after the smart rock had been deployed. Finally, the smart rock SR1 was located from the collected data.

Figure 1 I-44W Roubidoux Creek Bridge

A. Test Setup and Layout

All tests were conducted on the shoulder of bridge deck near Bent 7 (Pier 7) as shown in Figure 2(a, b). A total station was set near the Pier 8 on the Rolla side. The center of the total station was used as the origin of a Cartesian coordinate system XYZ with X-, Y-, and Z- axles defined along the transverse, longitudinal (traffic direction), and vertical (upward) directions, respectively. One smart rock, designed by SR1, was deployed on the Rolla side of Pier 7. The test crane was fixed on a trailer that was towed into predetermined positions by a truck. The magnetometer sensor mounted on the test crane was extended down from the bridge deck to measure the ambient magnetic field and the total magnetic field with the smart rock. Prism 3 mounted right below the sensor as shown in Figure 2(c) was used to represent the coordinate for each measurement. Prism 1 and 2 fixed at two ends of horizontal bar of the test crane were employed to ensure that the bar was paralleled to the X axis. The measurement points in XOY plane shown in Figure 2(a) were selected as cross points in mesh 1 for Pier 7. Mesh 1 was then translated to mesh 2 on the bridge deck for representative positions of the crane (specifically forklift) during tests, as illustrated in Figure 2(d). For each point in XOY plane, seven elevations denoted as Z1, Z2, Z3, Z4, Z5, Z6 and Z7 with equal spacing of 0.3 m were positioned for measurements in Z-direction. Therefore, a total of 42 measurement points for SR1 was taken around Bent 7. The total station set near Pier 8 was used to survey coordinates (location) of the smart rock and the magnetometer sensor positions as ground true data.

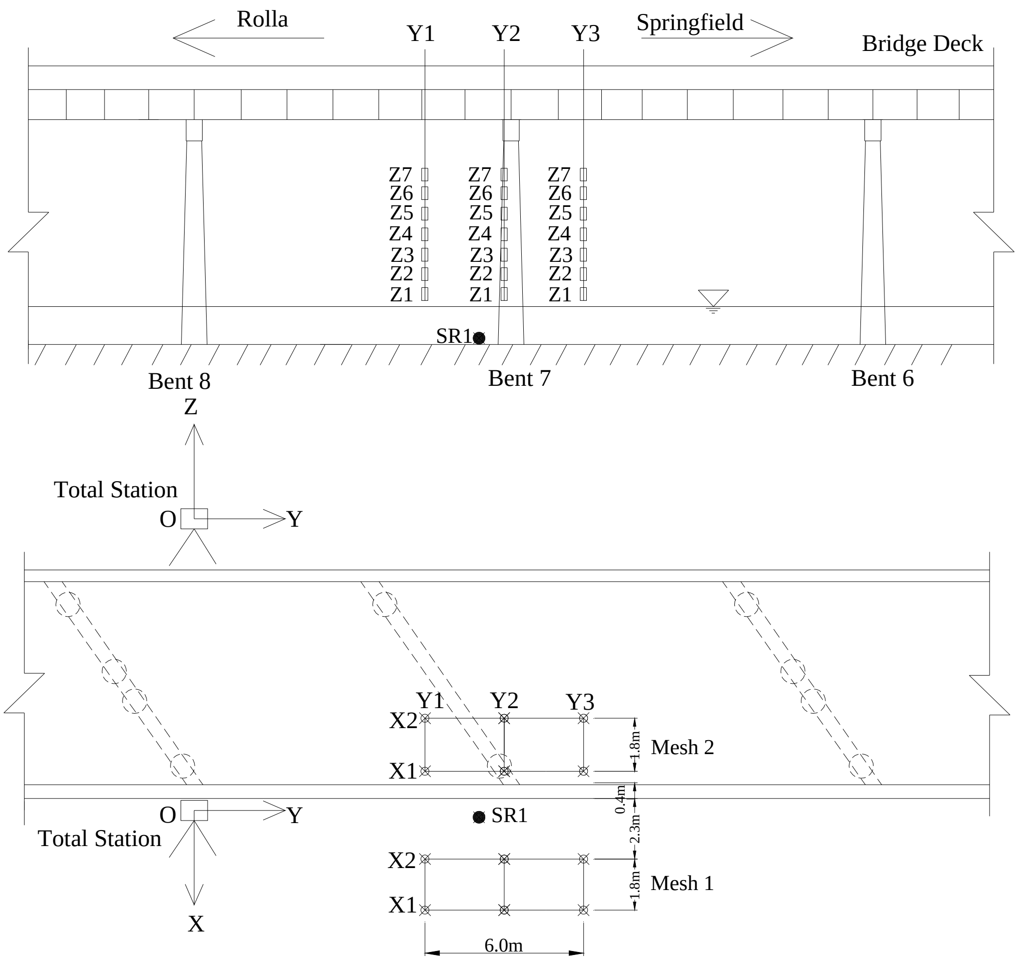

(a) Schematic View of Smart Rock and Sensor Locations in Plane

(b) Overview of the Entire Measurement System

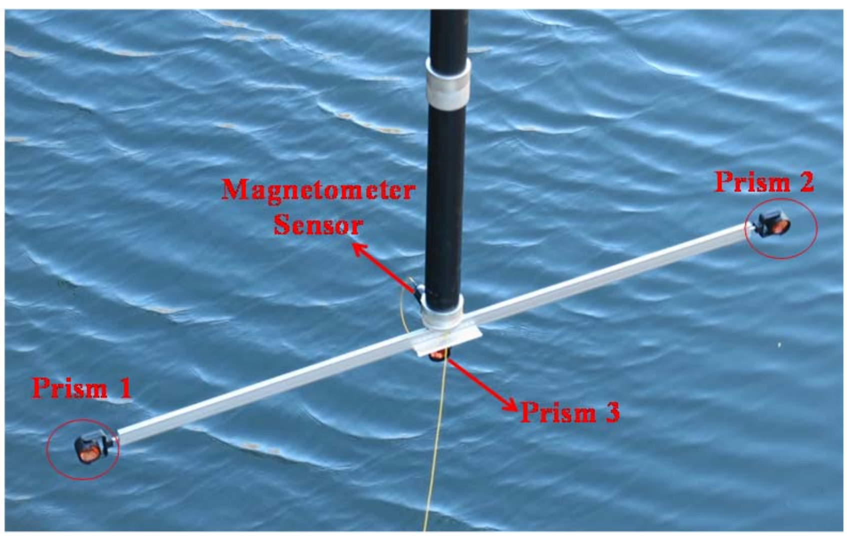

(c) Sensor ang Prism Positions

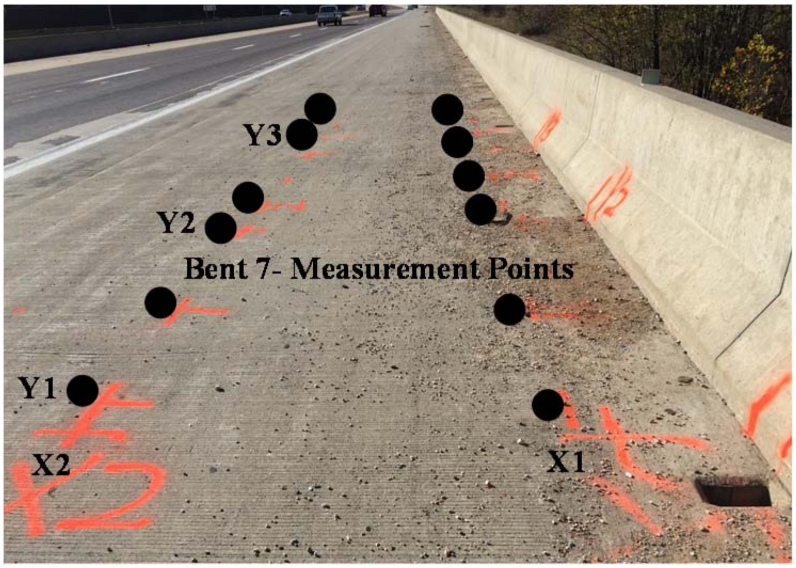

(d) Measurement Points Arrangement on Bridge Deck
Figure 2 Test Setup at the I-44W Roubidoux Creek Bridge Ssite

B. Test Procedures

(1) ***Set the XYZ Coordinate System.*** Since the bridge deck between Bent 8 and Bent 6 is straight, the Y-axis can be selected along the longitudinal (traffic) direction of the bridge. Two points O and B were selected by hanging a plumb down from the bridge railing to the ground close to Pier 8 and the sand hill between Pier 6 and Pier 7. Then the straight line linked from point O to B was defined as the Y-axis. The total station was placed at point O for wide visibility to the measurement points. A prism placed at point B shot by the total station to define the Y-axis by setting the parameters of the total station. The final coordinate system OXY was so determined that the longitudinal direction pointing to Springfield is the Y-axis, the X-axis is perpendicular to the Y-axis and pointing to downstream in the horizontal plane, and Z-axis is upward according to the right hand rule. The permanent point A on Pier 9 was also surveyed for future test reference. Furthermore, the OXY system can be rapidly and easily set up by shooting Point B and defining as the Y-axis so that the coordinate measurements for all points can be kept in one system for various field tests in different dates.

(2) ***Assemble the Test Crane***. As shown in Figures 2(b), the forklift was first loaded on the open trailer and, together with other parts, transported from Rolla to the field site. The horizontal aluminum alloy arm assembled in advance was then connected to the forklift on site. Next, nine carbon fiber tubes of 1.0 meter each were linked one by one and extended to the predetermined measurement points. Finally, the horizontal beam equipped with a magnetometer sensor and three prisms was mounted to the bottom of the carbon tube.

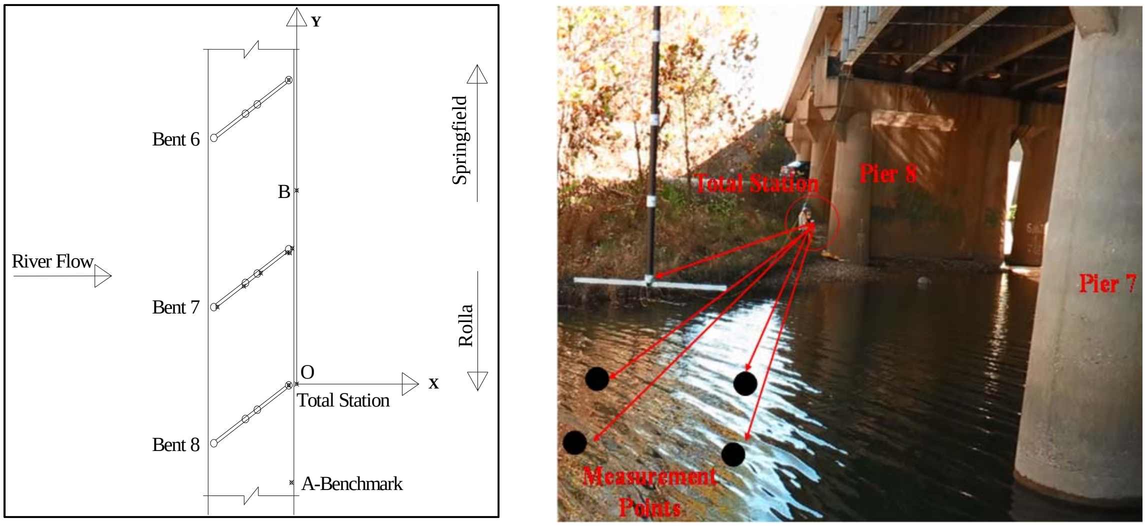

Figure 3 The Coordinate System Selection

(3) ***Set up the STL Digital Magnetometer***. As shown in Figure 2(b), the software exclusive for the sensor installed on the laptop controls the entire measurement process of the magnetic field. The Ethernet cable was used to transmit a signal from the sensor to the laptop by an interface called mini Ethernet box. The power for the sensor and laptop were provided by two commercial power boxes with rechargeable battery.

(4) ***Measure the Ambient Magnetic Field (AMF)***. The ambient magnetic field generated by the Earth and nearby ferromagnetic objects was measured prior to the deployment of any smart rock. As shown in Figure 2(a, b, d), the trailer made three stops in Y-direction and two stops in X-direction. At each of a total of six stops, seven movements in Z-direction were made by lifting up or lowering down the forklift. Figure 4(a) shows that the forklift positioned at Y2X1 and Y3X1 was realized by stopping the front and rear tire of the trailer at the marked points. At each marked point, the coordinate and magnetic intensity were collected simultaneously for each elevation in Z direction. The entire measurement sequence is given in Figure 4(b).

(a) Test Crane Located at Y2X2 and Y3X2

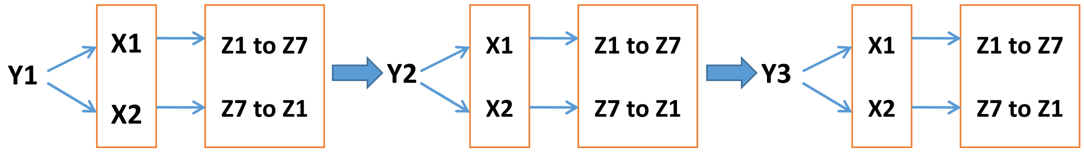

(b) Measurement Point Sequence Arrangement

Figure 4 Plan for Ambient Magnetic Field Measurements

(5) ***Deploy Smart Rock.*** As designed in the previous report, one smart rock (SR1) with two stacked N42 magnets in APUS configuration was embedded in concrete encasement as shown in Figure 5. The smart rock was transported in a boat from river bank and deployed at the downstream Rolla side of Pier 7 as illustrated in Figure 6. The smart rock can be observed from the sand hill close to Pier 7 with the rope floated on the water surface.

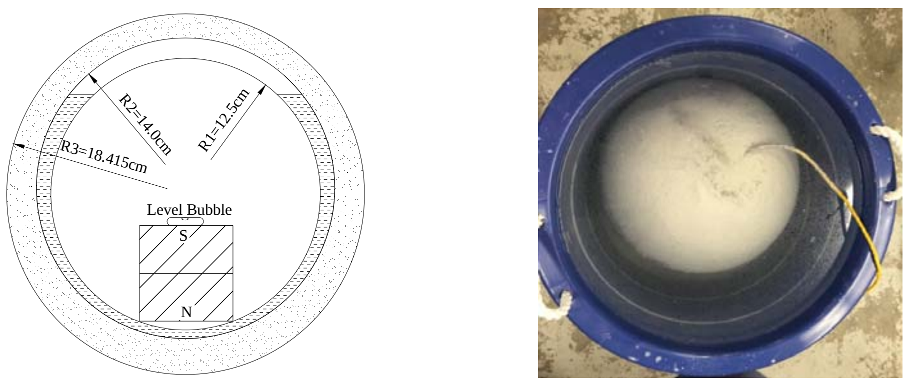

(a) Schematic View (b) Prototype

Figure 5 The Full-Scale Smart Rock

(a) Schematic View of SR1 (b) Deployment of SR1

Figure 6 Arrangement and Deployment of Smart Rock

(6) ***Measure the Coordinate of Smart Rock***. The coordinate of the smart rock, SR1, was measured with the total station through the prism placed on the smart rock for ground truth data.

(7) ***Measure the Total Magnetic Field***. After the smart rock had been deployed, the total magnetic field (the combined effect of the smart rock, the Earth, and surrounding ferromagnetic substances) was measured following the same procedure as used for the AMF measurement. In this case, the total number of measurement points was also 42 around Pier 7 for SR1.

D. Localization Algorithm

Eqs. (1) and (2) represent the relationship among the total magnetic field intensity (B), the ambient field (B_{XA}, B_{YA} and B_{ZA}), and the magnetic field of a smart rock at coordinate (X_M, Y_M, Z_M). Both the (B_{XA}, B_{YA} and B_{ZA}) and the ($B_{XM}+B_{XA}$, $B_{YM}+B_{YA}$ and $B_{ZM}+B_{ZA}$) were measured at each point with coordinates (X,Y, Z). The objective error function represented by Eq. (3) was minimized through an appropriate optimization algorithm to numerically solve for the location of the smart rock or the (X_M, Y_M, Z_M) coordinate.

$$B=\sqrt{(B_{XM}+B_{XA})^2+(B_{YM}+B_{YA})^2+(B_{ZM}+B_{ZA})^2} \tag{1}$$

$$\begin{pmatrix} B_{XM} \\ B_{YM} \\ B_{ZM} \end{pmatrix} = \begin{pmatrix} -k\dfrac{3(Z-Z_M)(X-X_M)}{\left(\sqrt{(X-X_M)^2+(Y-Y_M)^2+(Z-Z_M)^2}\right)^5} \\ -k\dfrac{3(Z-Z_M)(Y-Y_M)}{\left(\sqrt{(X-X_M)^2+(Y-Y_M)^2+(Z-Z_M)^2}\right)^5} \\ -k\dfrac{2(Z-Z_M)^2-(X-X_M)^2-(Y-Y_M)^2}{\left(\sqrt{(X-X_M)^2+(Y-Y_M)^2+(Z-Z_M)^2}\right)^5} \end{pmatrix} \tag{2}$$

$$J(X_M,Y_M,Z_M)=\sqrt{\sum_{i=1}^{n}[B_i^{(P)}-B_i^{(M)}]^2} \tag{3}$$

E. Test Results and Discussion

Table 1 summarizes the coordinates of 42 measurement points, the AMF intensities prior to deployment of the smart rock, and the total intensities after deployment of the smart rock SR1. The coefficient *k* for the N42 magnet is calculated from the maximum residual flux density. The three components of the total magnetic field (B_x, B_y, B_z) were directly measured from the 3-axis flux magnetometer in which three directions marked on the sensor was placed exactly parallel to the three axles of the O-XYZ coordinate system. Therefore, the three components of the total magnetic field and the three components ($B_{Ax,}$ B_{Ay} and B_{Az}) of the ambient magnetic field were substituted into the localization algorithm to determine the coordinates of the smart rock SR1.

Table 1 Coordinates and Intensities of Measurement Points for SR1

Measurement Point		Measurement Points Coordinate (m)			N42 Magnet Factor ($nT.m^3$)	AMF Intensity (nT)				SR1 & AMF Intensity (nT)			
		X_i	**Y_i**	**Z_i**	***k***	**B_{Ax}**	**B_{Ay}**	**B_{Az}**	**B_A**	**B_x**	**B_y**	**B_z**	**B**
Y1X1	Z1	3.854	21.793	-1.002	86521	22781	1016	-48909	53964	21379	-827	-48734	53224
	Z2	3.822	21.612	-0.701	86521	22408	1742	-49004	53912	21574	306	-48788	53346
	Z3	3.807	21.631	-0.408	86521	22418	2230	-48950	53886	21712	171	-48842	53451
	Z4	3.814	21.673	-0.116	86521	22444	2370	-48912	53868	21898	91	-48852	53536
	Z5	3.794	21.560	0.189	86521	22411	2321	-48907	53847	22060	450	-48867	53618
	Z6	3.785	21.510	0.489	86521	22866	3345	-48673	53880	22142	618	-48903	53685
	Z7	3.834	21.554	0.795	86521	22631	2399	-48778	53826	22073	253	-48957	53703
Y1X2	Z1	2.068	21.869	-0.993	86521	22776	1666	-48933	53999	18988	6554	-49341	53274
	Z2	2.060	21.780	-0.721	86521	22776	1666	-48933	53999	19357	6669	-49660	53715
	Z3	2.062	21.810	-0.402	86521	22457	2795	-49110	54074	19662	6608	-49931	54069
	Z4	1.995	21.665	-0.099	86521	22452	2864	-49181	54140	20196	7012	-49988	54367
	Z5	2.068	21.700	0.190	86521	22402	2711	-49292	54211	20420	7785	-50010	54576
	Z6	2.080	21.632	0.469	86521	22457	2934	-49382	54328	20525	7090	-50204	54699
	Z7	2.083	21.606	0.781	86521	22496	3237	-49477	54447	21054	7653	-50118	54896
Y2X1	Z1	3.839	24.512	-0.995	86521	22469	2162	-48734	53708	21434	-814	-48329	52875
	Z2	3.833	24.495	-0.740	86521	22555	2478	-48613	53648	21426	51	-48434	52961
	Z3	3.805	24.416	-0.392	86521	22413	2543	-48621	53598	21527	788	-48502	53070
	Z4	3.790	24.321	-0.110	86521	22883	2794	-48351	53565	21649	874	-48562	53176
	Z5	3.801	24.393	0.180	86521	22367	2796	-48550	53528	21778	818	-48604	53266
	Z6	3.798	24.371	0.473	86521	22478	2709	-48476	53502	21785	628	-48679	53335
	Z7	3.788	24.293	0.778	86521	22349	2785	-48505	53479	22325	1627	-48499	53416
Y2X2	Z1	2.068	24.565	-0.997	86521	22948	4410	-47983	53371	19115	3895	-48826	52578
	Z2	2.007	24.451	-0.713	86521	22847	4933	-47848	53252	19417	4931	-49317	53231
	Z3	2.036	24.490	-0.403	86521	22678	5684	-47809	53219	19613	5190	-49598	53587
	Z4	2.035	24.483	-0.114	86521	22333	5235	-48189	53370	19816	5444	-49792	53866
	Z5	2.028	24.400	0.190	86521	22328	4955	-48373	53507	20274	6156	-49855	54171
	Z6	1.959	24.201	0.497	86521	22236	5194	-48555	53656	20529	6653	-49912	54377
	Z7	2.076	24.302	0.799	86521	22296	5549	-48660	53812	20415	6696	-50034	54452
Y3X1	Z1	3.843	27.686	-1.025	86521	21490	2251	-48990	53543	21569	801	-48624	53199
	Z2	3.840	27.665	-0.743	86521	21543	2402	-48947	53532	21631	683	-48627	53226
	Z3	3.785	27.590	-0.407	86521	21576	2687	-48907	53523	21566	705	-48693	53259
	Z4	3.840	27.581	-0.122	86521	21746	2526	-48835	53518	21764	1297	-48602	53269
	Z5	3.836	27.552	0.188	86521	21859	2742	-48733	53481	21642	613	-48713	53308
	Z6	3.850	27.522	0.465	86521	21776	2584	-48782	53485	21864	727	-48643	53336
	Z7	3.840	27.452	0.760	86521	21761	3392	-48689	53439	21876	817	-48643	53342

	Z1	2.128	27.594	-1.018	86521	20843	5225	-49284	53765	20334	5057	-48970	53264
	Z2	2.106	27.299	-0.716	86521	20890	5285	-49272	53778	20457	5283	-49004	53364
	Z3	2.037	27.213	-0.409	86521	21078	5449	-49203	53805	20740	6488	-48828	53445
Y3X2	Z4	2.035	27.313	-0.116	86521	21050	5374	-49273	53850	20931	6634	-48882	53587
	Z5	2.033	27.263	0.193	86521	21279	5359	-49249	53917	20944	6050	-49127	53746
	Z6	2.093	27.355	0.471	86521	21534	5792	-49124	53948	20905	5735	-49332	53884
	Z7	2.081	27.299	0.758	86521	21700	6878	-48975	54006	20987	6774	-49288	53997

Table 2 Predicted and Measured Location of SR1

	X_M/m	Y_M/m	Z_M/m
Predicted SR1 Location	0.063	23.491	-3.032
Measured SR1 Location	0.089	23.235	-3.042
Location Prediction Error for SR1	0.026	0.256	-0.010
SRSS Error in Coordinate	0.258 m		

Table 2 compares the predicted and measured coordinates (X_M, Y_M, Z_M) of the smart rock SR1. It can be observed that the largest component error of 25.6 cm occurred in Y coordinate mainly due to inaccurate positioning of the prism for SR1 surveying when a measurement bar was intended to be placed at the center top of the smart rock with 36.83 cm in diameter. The square-root-of-the-squared-sum (SRSS) prediction error is 25.8 cm, which is acceptable within an error limit of 50 cm targeted at the beginning of this project. Therefore, the smart rock localization algorithm is accurate.

Task 3.2 Visualization Tools for Rock Location Mapping over Time

The 999ci HD KVD SI Combo – Sonar instrument with side imaging from Humminbird was used to map the river bed profile around the studied pier. The side image can show any structures, timber, wrecks, falling logs and fish on the river bed under the water. The included GPS chart plotting with built-in Humminbrid ContourXD map can provide the track lines and the position of the boat.

As shown in Figure 7(a), the sonar transducer was attached on one side of the boat and submerged in water below the bottom of the boat. The control head of the sonar connected to the transducer was operated to map the river bed profile and location of the rock. The boat was planned to first pass through the studied pier as close as possible along the water current to collect clear information around the pier. Then, another straight pass was made away from the pier along current direction in order to map the river bed. Figure 7(b) illustrates the boat equipped with the sonar instrument passing through the bridge pier.

(a) Sonar Instrument Installation (b) Operation on the Boat

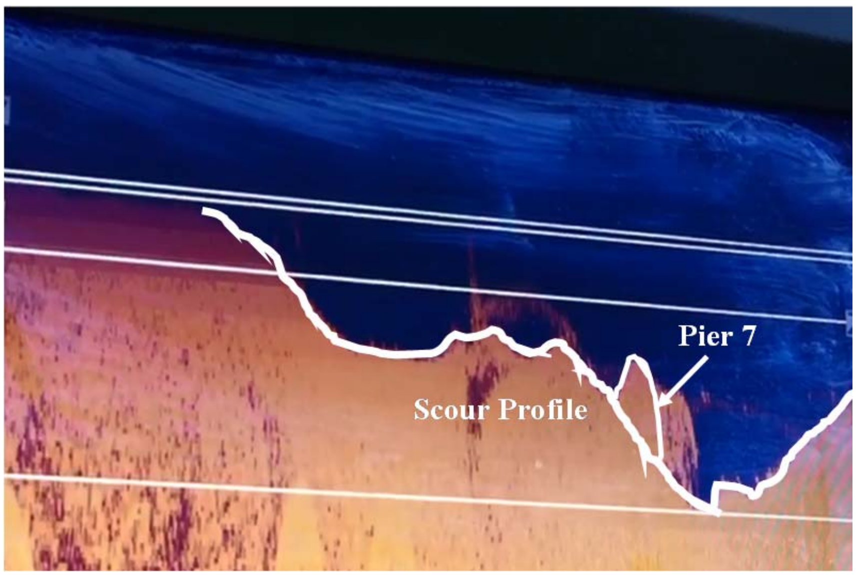

(c) The Scour Profile around Pier 7

Figure 7 The Sonar Instrument and River Bed Profile

A snapshot of the sonar screen as shown in Figure 7(c) was taken during the operation, in which the scour profile around Pier 7 can be seen. The smart rock should be located on the river bed downstream side about 1 m away from Pier 7. The smart rock was not shown up on the sonar screen likely because the travel route or the orientation of the transducer deviated from the smart rock.

Task 4 Technology Transfer, Report and Travel Requirements - Quarterly Report Submitted, Travel Completed, or Meeting Conducted

The 5st quarterly report is being submitted.

I.2 PROBLEMS ENCOUNTERED

In this quarter, smart rock deployment was postponed due to the late arrival of the custom-made test crane.

I.3 FUTURE PLAN

The following task and subtasks will be executed during the next quarter.

Task 3.1 Time- and Event-based Field Measurements

More field tests at bridge sites in Missouri and/or California will be conducted to validate the localization of smart rocks. In particular, during or after a flood event, the team would like to make field measurements provided traffic control is made available.

Task 3.2 Visualization Tools for Rock Location Mapping over Time - Software Completed & Tested

This task will continue based on the field test results.

Task 4 Technology Transfer, Report and Travel Requirements - Quarterly Report Submitted, Travel Completed, or Meeting Conducted

The 6th quarterly report will be prepared and submitted.

.

II – BUSINESS STATUS

II.1 HOURS/EFFORT EXPENDED

The planned hours and the actual hours spent on this project are given and compared in Table 3. In the fifth quarter, the actual hours are more than the planned hours by 27%, leading to an actual cumulative hour of approximately 135% of the planned hours. (Note: there were significant errors in the planned labor hours stated in the previous reports.) The cumulative hours spent on various tasks by personnel are presented in Figure 8.

Table 3 Hours Spent on This Project

	Planned		Actual	
	Labor Hours	Cumulative	Labor Hours	Cumulative
Quarter 1	236	236	176	176
Quarter 2	236	472	294	471
Quarter 3	236	708	294	765
Quarter 4	236	944	566	1331
Quarter 5	236	1180	300	1588
Quarter 6				
Quarter 7				
Quarter 8				

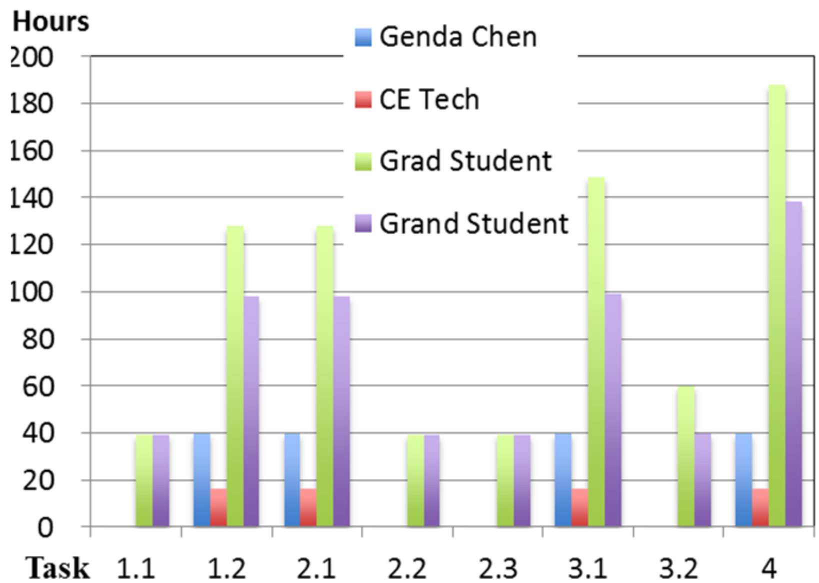

Figure 8 Cummulative Hours Spent on Various Tasks by Personnel

II.2 FUNDS EXPENDED AND COST SHARE

The budgeted and expended OST-R funds accumulated by quarter are compared in Figure 9. Approximately 117% of the budget has been spent till the end of fifth quarter. The actual cumulative expenditures from OST-R and MS&T/MoDOT are compared in Figure 10. The expenditure from OST-R is below the combined amount from the MS&T and MoDOT.

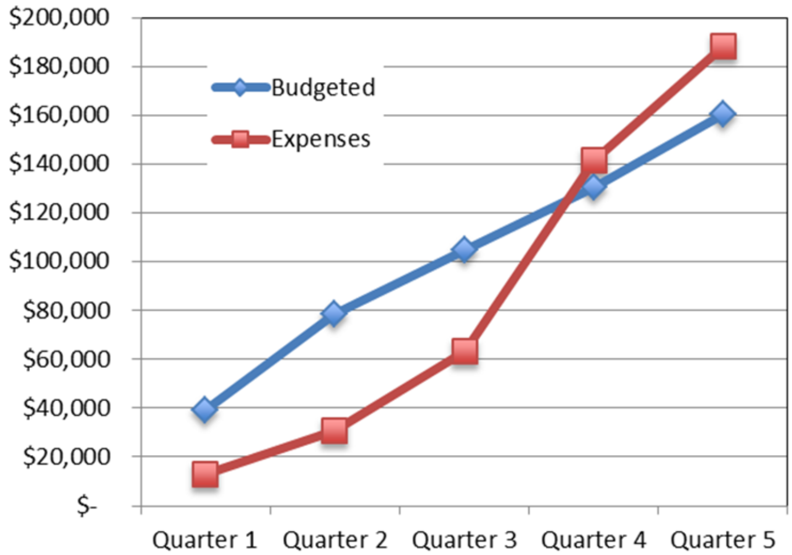

Figure 9 Comparison of OST-R Budget and Expenditure Accumulated by Quarter

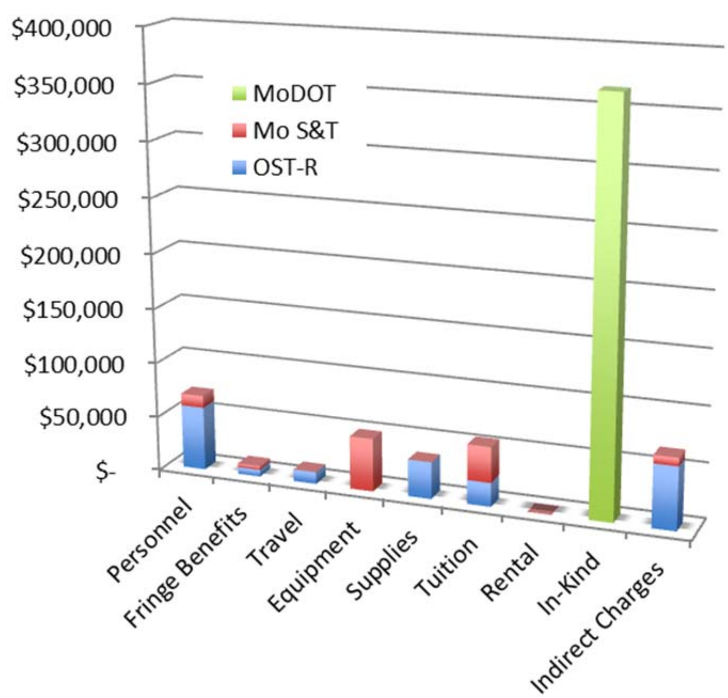

Figure 10 Cummulative Expenditures by Sponsor